

1 **3D8, a nucleic acid-hydrolyzing scFv, confers antiviral activity**
2 **against SARS-CoV-2 and multiple coronaviruses *in vitro***

3
4 Gunsup Lee^{1¶}, Shailesh Budhathoki^{2¶}, Hyeok Soon Choi^{1,3}, Kwang-ji Oh¹, Geum-Young Lee⁴, Yeon
5 Kyoung Ham¹, Young Jun Kim¹, Ye Rin Lim^{1,3}, Phuong Thi Hoang⁵, Yongjun Lee⁵, Seok-Won Lim⁶, Jun-
6 Mo Kim⁶, Seungchan Cho⁴, Jin-Won Song⁴, Sukchan Lee^{5*} and Won-Keun Kim^{2,3*}

7
8 ¹ Novelgen Co., Ltd., R&D center, 77, Changnyong-daero 256 beon-gil, Yeongtong-gu, Suwon-si,
9 Gyeonggi-do, Republic of Korea

10 ² Department of Microbiology, College of Medicine, Hallym University, Seoul, Republic of Korea

11 ³ Institute of Medical Science, College of Medicine, Hallym University, Chuncheon, Republic of Korea

12 ⁴ Department of Microbiology, Korea University College of Medicine, Seoul, Republic of Korea

13 ⁵ College of Biotechnology and Bioengineering, Sungkyunkwan University, Suwon, Republic of Korea

14 ⁶ Animal Functional Genomics & Bioinformatics Lab., Department of Animal Science and Technology,
15 Chung-Ang University, Anseong, Gyeonggi-do, Republic of Korea

16
17 *Corresponding author

18 Email: wkkim1061@hallym.ac.kr (W-KK) and cell4u@skku.edu (S-CL)

19
20 ¶These authors contributed equally to this work.

25 **Abstract**

26 The current pandemic severe acute respiratory syndrome coronavirus 2 (SARS-CoV-2) pose a
27 critical public health threat worldwide. Coronaviruses (subfamily Orthocoronavirinae, family
28 Coronaviridae, order Nidovirales) are a group of enveloped positive-sense single-stranded RNA
29 viruses. Six pathogenic human coronaviruses, likely zoonotic viruses, cause the common cold in
30 humans. A new emerging coronavirus, SARS-CoV-2, become a crucial etiology for the
31 Coronavirus-induced disease 19 (COVID-19). However, effective therapeutics and vaccines
32 against multiple coronaviruses remain unavailable. This study aimed to investigate an antiviral
33 molecule, single chain variable fragment (scFv), against SARS-CoV-2 and other coronaviruses.
34 3D8, a recombinant scFv, exhibits broad-spectrum antiviral activity against DNA and RNA viruses
35 owing to its nucleic acid-hydrolyzing property. Here, we report that 3D8 scFv inhibited the
36 replication of SARS-CoV-2, human coronavirus OC43 (HCoV-OC43), and porcine epidemic
37 diarrhea virus (PEDV). Our results revealed the prophylactic and therapeutic effects of 3D8 scFv
38 against SARS-CoV-2 in Vero E6 cells. Immunoblot and plaque assays showed the absence of
39 coronavirus nucleoproteins and infectious particles in 3D8 scFv-treated cells, respectively. In
40 addition, we observed the antiviral effects of 3D8 against HCoV-OC43 and PEDV. In conclusion,
41 this study provides insights into the broad-spectrum antiviral agent of 3D8 scFv; thus, it could be
42 considered a potential antiviral countermeasure against SARS-CoV-2 and zoonotic coronaviruses.

43

44 **Key points (Main message):**

- 45 1. 3D8, a nucleic acid-hydrolyzing scFv, exhibits potent prophylactic and therapeutic
46 antiviral effects on SARS-CoV-2.

47 2. 3D8 exhibits broad-spectrum antiviral activity against multiple coronaviruses: hCoV OC43
48 and PEDV.

49 3. 3D8 potentially degrades viral RNA.

50

51 **Introduction**

52 Coronaviruses (subfamily Orthocoronavirinae in the family Coronaviridae of the order
53 Nidovirales) belong a group of enveloped viruses containing a single-stranded positive-sense RNA
54 genome (1, 2). Divergent coronaviruses constitute four genetic lineage groups, including
55 alphacoronaviruses, betacoronaviruses, gammacoronaviruses, and deltacoronaviruses. These
56 viruses infect a broad range of natural reservoir hosts, including humans, bats, rodents, pigs, and
57 camels (3). Currently, six coronavirus species cause infectious diseases in humans. Four
58 coronaviruses, human coronavirus OC43 (HCoV-OC43), 229E, NL63, and HKU1, induce flu-like
59 common cold symptoms in immunocompromised individuals (4, 5). Two highly transmissible and
60 pathogenic viruses, severe acute respiratory syndrome coronavirus 1 (SARS-CoV-1) and Middle
61 East respiratory syndrome coronavirus (MERS-CoV), are associated with fatal illness involving
62 pneumonia and respiratory disorders (6). In late December 2019, the city of Wuhan, in the Hubei
63 province of China, reported a few cases of patients with severe pneumonia of an unknown
64 etiological agent (7), which was identified as the novel coronavirus disease (COVID-19) caused
65 by SARS-CoV-2 (8). SARS-CoV-2 has several similarities to SARS-CoV and binds to the
66 common host cell receptor, angiotensin-converting enzyme 2 (ACE-2), and Transmembrane
67 Serine Protease 2 (TMPRSS2) (9, 10); however, the novel strain is genetically distinct from SARS-
68 CoV-1 (11). The novel coronavirus SARS-CoV-2 is transmitted through species barriers from bats
69 to humans (12). COVID-19 is characterized by influenza-like symptoms ranging from mild to

70 severe lung injury as well as multi-organ failure, leading to death in patients with comorbidities
71 (13). This novel virus has led to a global pandemic, which resulted in unparalleled public health
72 emergencies (14). As of November 24, 2020, it has rapidly spread to 220 countries and territories,
73 infecting over 58.7 million people including more than 1.38 million deaths (15)
74 [<https://covid19.who.int>].

75 The rapid and widespread emergence of SARS-CoV-2 presents the urgent need for antiviral
76 countermeasures (4). Currently, there are no available therapeutics against human coronaviruses.

77 A variety of antivirals are repositioning on clinical trials Nucleoside analogues (remdesivir,
78 favipiravir and ribavirin), protease inhibitors (disulfiram, lopinavir and ritonavir), antiparasitic
79 drugs (chloroquine and hydrochloroquine), pegylated interferons, monoclonal antibodies,
80 oligonucleotide-based therapies, peptides and small-molecule drugs are contemplated for possible
81 therapeutic agents against SARS-CoV-2 (16, 17). In particular, remdesivir, which inhibits viral
82 RNA polymerases, is proposed as a potent antiviral against SARS-CoV-2 and clinical
83 improvement has been observed in patients under compassionate use (18, 19)

84 3D8, a 27-kDa recombinant antibody fragment, is a single chain variable fragment (scFv) that
85 comprises a variable region of a heavy chain covalently linked to the corresponding variable region
86 of a light chain. It was originally found in autoimmune-prone Murphy Roths Large (MRL) mice
87 (20). The 3D8 scFv possessing the nucleic acid hydrolyzing activity degrades viral DNA and/or
88 mRNA in the infected cells (21, 22). This protein has the broad-spectrum antiviral effects against
89 herpes simplex virus (HSV), influenza virus, and pseudorabies (PRV) virus *in vitro*. 3D8 exhibited
90 *in vivo* antiviral therapeutic effects against PRV in C57BL/6 mice. The transmission of avian
91 influenza and bronchitis viruses was suppressed in transgenic chickens expressing the 3D8 scFv

92 (23-26). However, the antiviral activity of the 3D8 scFv against SARS-CoV-2 and other
93 coronaviruses remains unknown.

94 Here, this study aimed to investigate the antiviral activity of 3D8 scFv against emerging
95 coronaviruses *in vitro*. These data provide insight into a broad-spectrum antiviral agent of scFv
96 against SARS-CoV-2 and multiplex coronaviruses.

97

98 **Results**

99 **3D8 inhibits SARS-CoV-2 in a dose-dependent manner**

100 To determine the antiviral activity of the 3D8 scFv against SARS-CoV-2, different concentrations
101 of the scFv were applied to Vero E6 cells after virus challenge. SARS-CoV-2 replication in cultures
102 treated with various doses of 3D8 was quantified using RT-qPCR (**Fig 1A**). The replication of
103 SARS-CoV-2 significantly decreased in a 3D8 dose-dependent manner. The 10 μ M and 5 μ M
104 concentrations of 3D8 effectively inhibited viral replication by up to approximately 90% and 75%,
105 respectively, compared to the non-treatment group. The production of infectious virus particles was
106 quantified by performing the plaque assay (**Fig 1B**). The viral titer of SARS-CoV-2 was reduced in
107 a 3D8 dose-dependent manner. In particular, when treated with 10 μ M of 3D8, the titer of the virus
108 was reduced by 10 times compared to the non-treatment group. Continual treatment with 3D8
109 showed antiviral activity against SARS-CoV-2 at an effective concentration (EC50) of 4.25 μ M
110 (**Fig 1C**). Moreover, this scFv did not show cytotoxicity in Vero E6 cells treated with the 3D8 scFv
111 at concentrations ranging from 1 μ M to 10 μ M (**Fig 1D**). However, cytotoxicity was noted at a dose
112 of 40 μ M.

113

114 **3D8 effectively inhibits SARS-CoV-2 in pretreated cells (prophylactic effect)**

115 We determined the prophylactic antiviral activity of the 3D8 scFv against SARS-CoV-2 in
116 pretreated cell cultures. A significant reduction in the SARS-CoV-2 N gene copies was observed
117 upon treatment with 10 μ M 3D8 scFv (**Fig 2A**). The gene copy number of the SARS-CoV-2 E gene
118 and RdRp gene was reduced by 99.6% and 99.4%, respectively (data not shown). The N protein of
119 SARS-CoV-2 was not observed after treatment with the 3D8 scFv (**Fig 2B**). Furthermore, we
120 determined the inhibitory effect of 3D8 on the production of infectious particles of SARS-CoV-2.
121 The production of infectious virus particles was more than 10 times lower in the scFv-treated group
122 than in the control group (**Fig 2C**). Collectively, these data demonstrated that 3D8 has a
123 prophylactic effect on SARS-CoV-2 infection.

124

125 **3D8 effectively inhibits SARS-CoV-2 in post-treated cells (therapeutic effect)**

126 To determine the therapeutic effect of 3D8 at 2 h post-infection (p.i.), we assessed the inhibitory
127 activity of SARS-CoV-2 based on the reduction of the relative gene copy number (**Fig 2D**). 3D8
128 treatment resulted in a decrease in the gene copy number of the N gene by 63.4%. Western blot
129 analysis revealed the absence of N protein expression in the 3D8-treated samples (**Fig 2E**). The
130 production of infectious particles of SARS-CoV-2 in the 3D8-treated group was 10 times lower
131 than that in the control group (**Fig 2F**). The reduced viral gene copy number, lack of infectious
132 virus particles, and absence of N protein expression indicated the therapeutic effect of 3D8 upon
133 SARS-CoV-2 infection.

134

135 **3D8 possesses broad-spectrum antiviral activity against multiple coronaviruses**

136 To determine the antiviral activity of 3D8 against other coronaviruses, viral gene copies and
137 infectious particles were examined after HCoV-OC43 and PEDV infections. The 3D8-treated group

138 revealed effective inhibition of viral replication upon HCoV-OC43 infection. The load of HCoV-
139 OC43 RNA was significantly reduced in a 3D8 dose-dependent manner (**Fig 3A**). The expression
140 of viral proteins was inhibited upon treatment with 3D8 (**Fig 3B**). 3D8 effectively inhibited the
141 replication of HCoV-OC43 with the EC₅₀ value of 1.40 μM (**Fig 3C**). Immunohistochemistry
142 analysis exhibited a reduction in HCoV-OC43 replication upon 3D8 treatment (**Fig 3D**).
143 Treatment with 3D8 resulted in the effective inhibition of viral replication upon PEDV infection.
144 The load of PEDV RNA was significantly suppressed in a 3D8 dose-dependent manner (**Fig 4A**).
145 The expression of viral proteins was reduced upon treatment with 3D8 (**Fig 4B**). The EC₅₀ value of
146 3D8 against PEDV was 1.10 μM (**Fig 4C**). Immunohistochemistry analysis revealed a reduction in
147 PEDV replication upon 3D8 treatment (**Fig 4D**). These data demonstrated the broad-spectrum
148 activity of 3D8 against multiple zoonotic coronaviruses.

149

150 **Discussion**

151 Three novel human coronaviruses have emerged during the past two decades (3, 5). The outbreak
152 of COVID-19 occurred in late December in Wuhan (China) and rapidly became a global pandemic
153 (7). The public health emergency caused by the SARS-CoV-2 outbreak presents the demand for
154 countermeasures against emerging and re-emerging zoonotic coronaviruses. As the virus
155 disseminates, efforts are being made to mitigate transmission via public health interventions
156 including social distancing, quarantine, and contact tracing. However, therapeutics and vaccines
157 against SARS-CoV-2 are urgently needed for the effective control of outbreaks. In this study, we
158 demonstrated that 3D8, a nucleic acid-hydrolyzing scFv, inhibited the replication of SARS-CoV-2
159 and multiple coronaviruses *in vitro*.

160

161 The scFv is a molecule derived from an antibody composed of variable region of heavy and light
162 chains linked with peptides(20). scFv has applied for basic researches, biotechnological and
163 medicinal applications such as cancer therapy and potential alternatives to conventional diagnostic
164 approaches(25, 26). scFv has various advantages over traditional monoclonal antibodies such as
165 ease of genetic manipulation, rapid molecular design and characterization, greatly reduced size,
166 production of antibodies against viral proteins, and various expression systems. Neutralizing scFv
167 against N protein protects piglets from PEDV infection (27). The orally administered piglets had
168 no or mild clinical symptoms, intestinal lesions and significantly increased survival rates. 3D8 is a
169 unique scFv that possesses a broad-spectrum nuclease activity and confers antiviral protection from
170 a variety of viruses including DNA and RNA viruses (**Figure 5**) (28, 29). 3D8 scFv previously
171 showed the antiviral effect against infectious Bronchitis virus, a member of gammacoronaviruses
172 in transgenic chickens expressing 3D8 scFv (24). The antiviral activity of 3D8 scFv against SARS-
173 CoV-2 and other coronaviruses remained to be examined.

174 Our study demonstrated that 3D8 confers effective antiviral activity against SARS-CoV-2, HCoV-
175 OC43, and PEDV *in vitro*. The function of 3D8 inhibited the replication of multiple coronaviruses
176 in a dose-dependent manner. The reduction of infectious virus particles accounted for the nuclease
177 activity of 3D8, indicating the degradation of viral nucleic acids prohibited the production of viral
178 genomes and proteins. Upon infection with HCoV-OC43 and PEDV, the therapeutic treatment of
179 3D8 scFv showed the inhibition of viral replication and protein expression, indicating the antiviral
180 activity of multiple coronaviruses. The previous studies demonstrated the biochemical
181 characteristics and robust antiviral activity of 3D8 scFv against classical swine fever virus and
182 herpes simplex virus *in vitro* (22, 28). The 3D8 expressing transgenic mice and chickens exhibited
183 the *in vivo* antiviral activity against influenza virus and PRV (23, 29). The cellular entry mechanism

184 of 3D8 revealed a caveolin-dependent manner without a carrier (30). The intranasal transfer of 3D8
185 scFv into a mouse described the presence of the protein in the epithelial barrier of lung tissues (31).
186 Taken together, the 3D8, a nucleic-acid hydrolyzing mini-antibody, may be a potential candidate
187 for antivirals due to the broad spectrum, the easy penetration to the cell, and the accessibility to the
188 lung *in vivo*.

189 Infection of coronaviruses have significantly impacted on humans and livestock (32). However,
190 the effective antiviral countermeasures against the viruses are still unavailable. HCoV-OC43,
191 belongs to lineage betacoronaviruses, is associated with mild common cold in humans. HCoV-
192 OC43 infection occurs frequently in early childhood and causes acute respiratory tract illness,
193 pneumonia and croup (33). PEDV, a member of alphacoronaviruses, is a highly contagious
194 coronavirus that causes severe diarrhea and death in neonatal piglets (27). All of age groups are
195 highly susceptible to PEDV infection with neonatal piglets under 2 weeks of age, showing the
196 highest mortality rates. In this study, HCoV-OC43 and PEDV were effectively reduced for the
197 replication and protein synthesis. These results suggest 3D8 may be a potential antiviral agent
198 against viral threats for the public health and livestock industry.

199 In this study, there is the limitation. The absence of *in vivo* study is a major limitation in animal
200 models. To address this, future studies are needed to illustrate the *in vivo* inhibitory effect of 3D8
201 scFv using the animal models. Although the previous studies presented the nuclease activity of 3D8
202 scFv, the precise cellular mechanism and *in vivo* effects of the administration remain to be further
203 investigated.

204 In conclusion, 3D8 scFv confers effective antiviral activity against the SARS-CoV-2 and multiple
205 coronaviruses. This study provides insights into the broad-spectrum antiviral countermeasure of
206 scFv; thus, it can be a potential antiviral agent against the emerging virus outbreak.

207

208 **Materials and methods**

209 **Ethics**

210 An antiviral study of 3D8 against SARS-CoV-2 was performed at the Biosafety Level-3 facilities
211 at Hallym Clinical and Translational Science Institute, Hallym University, Chuncheon, South
212 Korea, under guidelines and protocols approved by institutional biosafety requirements.
213 Experiments involving OC43 and PEDV were performed at Biosafety Level-2 facilities.

214

215 **Cells and viruses**

216 African green monkey kidney epithelial Vero cells (ATCC[®] CCL-81) and Vero E6 cells (ATCC[®]
217 CRL-1586) were maintained in Dulbecco's Modified Eagle's Medium (DMEM, Lonza, USA 12-
218 604F, BioWhittaker[®]) supplemented with 10% fetal bovine serum (FBS, Gibco, USA), 1% 10 mM
219 HEPES in 0.85% NaCl (Lonza, USA, 17-737E, BioWhittaker[®]), and 100 U/mL penicillin and 100
220 µg/mL streptomycin (Pen Strep, Gibco, USA, 15070-063). Cell cultures were maintained at 37 °C
221 and 5% CO₂. SARS-CoV-2 was obtained from the Korea Centers for Disease Control and
222 Prevention (KCDC). The virus was propagated in Vero E6 cells, and the infectious titer was
223 determined by plaque assay in Vero E6 cells. hCoV OC43 and PEDV were obtained from KCDC
224 and the Korean Animal and Plant Quarantine Agency (KAPQA), respectively.

225

226 **Plaque assay**

227 Vero E6 cells were plated at 1×10^6 cells per well in 6-well plates (Corning) and incubated at 37
228 °C with 5% CO₂. A confluent monolayer of cells was washed with phosphate-buffered saline (PBS,
229 Lonza, USA, BioWhittaker[®]), infected with ten-fold serial dilutions of viral suspension prepared in

230 serum-free maintenance media (DMEM only), and incubated at 37 °C. Following infection for 1 h
231 with intermittent shaking at 15-min intervals, the viral inoculum was aspirated, and overlay media
232 (DMEM/F12 media) containing 4% bovine serum albumin (BSA), 2 mM glutamine, 2.5% sodium
233 bicarbonate (NaHCO₃), 10 mM HEPES, 50 mg/mL DEAE dextran, 100 U/mL penicillin, 100
234 µg/mL streptomycin (Pen Strep), and 0.6% immunodiffusion-grade Oxoid agar was added. After
235 4–5 days of incubation at 37 °C with 5% CO₂, fixation with 4% paraformaldehyde (Biosesang,
236 F1119Z21 YR) was performed. After overnight incubation, the overlay agar media was flicked
237 using a metal spatula, and the plates were stained with crystal violet (0.1% crystal violet in 20%
238 methanol) for 10 min. Plaques were enumerated, and viral titers were quantified.

239

240 ***In vitro* antiviral activity**

241 Cells were seeded at 1×10^6 cells per well and allowed to adhere for 24 h at 37 °C with 5% CO₂ in
242 6-well plates (Corning). After incubation, the cells were washed twice with PBS, and the viruses
243 were adsorbed at different multiplicity of infection (MOI) for 2 h at 37 °C. The plates were manually
244 rocked to ensure uniform and efficient distribution of inoculum every 15–20 min. After adsorption,
245 the cells were treated with 3D8 at different concentrations (2-h post-infection treatment of 3D8).
246 About 1 mL of DMEM supplemented with 10% FBS and antibiotics was added to the cells, which
247 were then incubated. In case of pre-treatment, Vero E6 cells were treated with 3D8 and incubated
248 overnight before the virus challenge. At 48 hour post infection (hpi), supernatants and cells were
249 harvested. The samples were stored at -80 °C until use.

250

251 **Real-time quantitative polymerase chain reaction**

252 Total RNA was extracted using TRIzol (Ambion, Life Technologies). Reverse transcription of
253 RNA into cDNA was performed using a High Capacity RNA-to-cDNA kit (Applied Biosystems,
254 Thermo Fisher Scientific) according to the manufacturer's protocol. Briefly, 1 µg of RNA was used,
255 and cDNA was synthesized using an oligo deoxythymine (dT) kit. The reaction was performed at
256 37 °C for 60 min, followed by 95 °C for 5 min.

257 Viral RNA was quantified via real-time quantitative PCR (RT-qPCR) using a Power SYBR® Green
258 PCR Master Mix (Applied Biosystems, Thermo Fisher Scientific) with primers for SARS-CoV-2
259 and other coronaviruses and GAPDH as an endogenous control. Details of the primers used are
260 provided in the supplementary information.

261

262 **Cell viability assay**

263 Vero-E6 cells were seeded at 4×10^4 cells per well in 96-well plates and incubated for 24 h at 37
264 °C in a CO₂ atmosphere. NVG308 protein was applied from 1 µM to 40 µM; the cells were
265 incubated for 48 h at 37 °C. After incubation, 10 µL of MTT solution (Intron) was added to each
266 well, and the cells were incubated for 3 h. After adding 100 µL of DMSO, the viability of the Vero-
267 E6 cells was measured using a microplate reader at 595 nm.

268

269 **Immunoblot assays**

270 Cells were lysed using RIPA lysis buffer (Santa Cruz Biotechnology, SC-24948). Cell lysates were
271 subjected to 10% sodium dodecyl sulfate-polyacrylamide gel electrophoresis (SDS-PAGE) and
272 transferred to a nitrocellulose membrane using a wet method. After transmembrane transfer, the
273 lysates were incubated with primary antibodies (anti-SARS-CoV-2, Invitrogen, PA1-41098; anti-
274 PEDV, MEDIAN, #9191; anti-hCoV OC43, LS-bio, LS-C79764; and anti-hGAPDH rabbit IgG,

275 Sigma-Aldrich, MFCD01322099 and Abcam, ab9485) overnight at 4 °C and then incubated with
276 an anti-rabbit IgG-HRP conjugate for 1 h at room temperature. The membrane reaction with ECL
277 solution (Bio-Rad, 170-5061) was observed and confirmed via the chemiluminescence mode using
278 ImageQuant LAS 500 (GE).

279

280 **Immunocytochemistry**

281 Immunocytochemistry for identifying the antiviral effects of 3D8 against the coronaviruses was
282 conducted as described previously [36]. Vero E6 cells were seeded at 1.5×10^4 cells in an 8-well
283 chamber and incubated for 24 h. PEDV and hCoV-OC43 were infected at MOI = 0.002 and 0.02,
284 respectively, for 2 h. About 5 μ M (185 μ g/mL) of purified 3D8 and 1% P/S antibiotics
285 (Gibco,15140122) were added to DMEM media (Hyclone, SH30243.01) supplemented with 10%
286 FBS (Welgene gold serum, S-001-07), and the media was incubated at 37 °C with 5% CO₂. The
287 cells were washed with PBS and fixed for 15 min in ice-cold methanol at room temperature. The
288 cells were then permeabilized with permeabilization buffer (Biolegend, #421002) for 10 min at
289 room temperature. After blocking with 1% BSA + 0.3 M glycine (22.52 mg/mL) + PBST buffer
290 for 1 h at room temperature, primary antibodies for detecting PEDV (mouse, anti-PEDV
291 monoclonal Ab, Mybio, #MBS313516), hCoV-OC43 (mouse, anti-OC43 monoclonal Ab, LSBio,
292 #LS-C79764), and 3D8 (polyclonal rabbit IgG Serum Ab) were incubated overnight at 4 °C.
293 Following this, PEDV and hCoV-OC43 were incubated with TRITC-conjugated anti-mouse Ab
294 (1:500) (Abcam, #ab6786), and 3D8 was incubated with Alexa 488-conjugated anti-rabbit Ab
295 (1:1000) (Abcam, #ab150077). The nuclei were stained with Hoechst (Thermo Fisher, #62249)
296 during the last 10 min of incubation at room temperature. Cells were mounted in mounting medium
297 (VECTASHIELD, #H-1200) and observed using a NIKON A1R (Eclipse A1Rsi and Eclipse Ti-E).

298

299 **Statistical analysis**

300 Statistical analyses of data were performed in Graph Pad Prism 8.

301

302 **Funding**

303 This work was supported by Novelgen (6R190101532S000100) and the Research Program To
304 Solve Social Issues of the National Research Foundation of Korea (NRF) funded by the Ministry
305 of Science and ICT (NRF-2017M3A9E4061992).

306

307 **Conflict of interest**

308 The authors declare that the research was conducted in the absence of any commercial or financial
309 relationships that could be construed as a potential conflict of interest.

310

311 **References**

- 312 1. S. H. Sun *et al.*, A Mouse Model of SARS-CoV-2 Infection and Pathogenesis. *Cell Host*
313 *Microbe*, (2020).
- 314 2. Y. Fan, K. Zhao, Z. L. Shi, P. Zhou, Bat Coronaviruses in China. *Viruses* **11**, (2019).
- 315 3. A. C. S. Timothy P. Sheahan, Shuntai Zhou, et al, An orally bioavailable broad-spectrum
316 antiviral inhibits SARS-CoV-2 in human airway epithelial cell cultures and multiple coronaviruses
317 in mice. *Science Translational Medicine* **12**, 15.
- 318 4. A. J. Pruijssers *et al.*, Remdesivir potently inhibits SARS-CoV-2 in human lung cells and
319 chimeric SARS-CoV expressing the SARS-CoV-2 RNA polymerase in mice. *bioRxiv*, (2020).

- 320 5. D. Blanco-Melo *et al.*, SARS-CoV-2 launches a unique transcriptional signature from *in*
321 *vitro*, *ex vivo* and *in vivo* systems. (2020).
- 322 6. X. Xie *et al.*, An Infectious cDNA Clone of SARS-CoV-2. *Cell Host Microbe* **27**, 841-848
323 e843 (2020).
- 324 7. N. Zhu *et al.*, A Novel Coronavirus from Patients with Pneumonia in China, 2019. *N Engl*
325 *J Med* **382**, 727-733 (2020).
- 326 8. J. Harcourt *et al.*, Severe Acute Respiratory Syndrome Coronavirus 2 from Patient with
327 Coronavirus Disease, United States. *Emerg Infect Dis* **26**, 1266-1273 (2020).
- 328 9. R. Lu *et al.*, Genomic characterisation and epidemiology of 2019 novel coronavirus:
329 implications for virus origins and receptor binding. *The Lancet* **395**, 565-574 (2020).
- 330 10. M. Hoffmann *et al.*, SARS-CoV-2 Cell Entry Depends on ACE2 and TMPRSS2 and Is
331 Blocked by a Clinically Proven Protease Inhibitor. *Cell* **181**, 271-280 e278 (2020).
- 332 11. Z. Chen *et al.*, From SARS-CoV to Wuhan 2019-nCoV Outbreak: Similarity of Early
333 Epidemic and Prediction of Future Trends. (2020).
- 334 12. A. E. Gorbalenya *et al.*, Severe acute respiratory syndrome-related coronavirus: The species
335 and its viruses – a statement of the Coronavirus Study Group. *Nature Microbiology*, 536-544
336 (2020).
- 337 13. V. Monteil *et al.*, Inhibition of SARS-CoV-2 Infections in Engineered Human Tissues
338 Using Clinical-Grade Soluble Human ACE2. *Cell* **181**, 905-913 e907 (2020).
- 339 14. A. B. Gussow *et al.*, Genomic determinants of pathogenicity in SARS-CoV-2 and other
340 human coronaviruses. *Proc Natl Acad Sci U S A* **117**, 15193-15199 (2020).
- 341 15. World Health Organization. (2020), vol. 2020.

- 342 16. G. Li, E. De Clercq, Therapeutic options for the 2019 novel coronavirus (2019-nCoV). *Nat*
343 *Rev Drug Discov* **19**, 149-150 (2020).
- 344 17. S. G. V. Rosa, W. C. Santos, Clinical trials on drug repositioning for COVID-19 treatment.
345 *Rev Panam Salud Publica* **44**, e40 (2020).
- 346 18. M. Wang *et al.*, Remdesivir and chloroquine effectively inhibit the recently emerged novel
347 coronavirus (2019-nCoV) *in vitro*. *Cell Res* **30**, 269-271 (2020).
- 348 19. A. J. Pruijssers *et al.*, Remdesivir Inhibits SARS-CoV-2 in Human Lung Cells and Chimeric
349 SARS-CoV Expressing the SARS-CoV-2 RNA Polymerase in Mice. *Cell Rep* **32**, 107940 (2020).
- 350 20. **M. H. Kwon** *et al.*, Production and Characterization of an anti-idiotypic single chain fv that
351 recognizes an anti-DNA antibody.pdf. *Immunological Investigations* **31**, 205-218.
- 352 21. Y. R. Kim *et al.*, Heavy and light chain variable single domains of an anti-DNA binding
353 antibody hydrolyze both double- and single-stranded DNAs without sequence specificity. *J Biol*
354 *Chem* **281**, 15287-15295 (2006).
- 355 22. H. R. Jun *et al.*, An RNA-hydrolyzing recombinant antibody exhibits an antiviral activity
356 against classical swine fever virus. *Biochem Biophys Res Commun* **395**, 484-489 (2010).
- 357 23. S. June Byun *et al.*, Transgenic Chickens Expressing the 3D8 Single Chain Variable
358 Fragment Protein Suppress Avian Influenza Transmission. *Sci Rep* **7**, 5938 (2017).
- 359 24. G. Lee *et al.*, The 3D8 single chain variable fragment protein suppress infectious bronchitis
360 virus transmission in the transgenic chickens. *Res Vet Sci* **123**, 293-297 (2019).
- 361 25. J. Lee *et al.*, Functional stability of 3D8 scFv, a nucleic acid-hydrolyzing single chain
362 antibody, under different biochemical and physical conditions. *Int J Pharm* **496**, 561-570 (2015).
- 363 26. Z. A. Ahmad *et al.*, scFv antibody: principles and clinical application. *Clin Dev Immunol*
364 **2012**, 980250 (2012).

- 365 27. F. Zhang *et al.*, Single Chain Fragment Variable (scFv) Antibodies Targeting the Spike
366 Protein of Porcine Epidemic Diarrhea Virus Provide Protection against Viral Infection in Piglets.
367 *Viruses* **11**, (2019).
- 368 28. G. Lee *et al.*, A nucleic-acid hydrolyzing single chain antibody confers resistance to DNA
369 virus infection in hela cells and C57BL/6 mice. *PLoS Pathog* **10**, e1004208 (2014).
- 370 29. G. Lee *et al.*, Therapeutic Strategy for the Prevention of Pseudorabies Virus Infection in
371 C57BL/6 Mice by 3D8 scFv with Intrinsic Nuclease Activity. *Mol Cells* **38**, 773-780 (2015).
- 372 30. J. Y. Jang *et al.*, A nucleic acid-hydrolyzing antibody penetrates into cells via caveolae-
373 mediated endocytosis, localizes in the cytosol and exhibits cytotoxicity. *Cell Mol Life Sci* **66**, 1985-
374 1997 (2009).
- 375 31. S. Cho *et al.*, Preventive Activity against Influenza (H1N1) Virus by Intranasally Delivered
376 RNA-Hydrolyzing Antibody in Respiratory Epithelial Cells of Mice. *Viruses* **7**, 5133-5144 (2015).
- 377 32. B. N. Fields, D. M. Knipe, P. M. Howley, *Fields' Virology*. (Wolters Kluwer
378 Health/Lippincott Williams & Wilkins, 2007).
- 379 33. R. Dijkman *et al.*, The dominance of human coronavirus OC43 and NL63 infections in
380 infants. *J Clin Virol* **53**, 135-139 (2012).

381

382 **Figure captions**

383 **Fig 1. 3D8 exhibits antiviral activity against SARS-CoV-2 in a dose-dependent manner**

384 (A) Dose-dependent inhibition of SARS-CoV-2 by 3D8. Vero E6 cells were infected with SARS-
385 CoV-2 and treated with a range of 3D8 concentrations at 2 hpi. At 48 hpi, the cells were harvested,
386 and the viral RNA level was determined using RT-qPCR. (B) Supernatants from the 3D8-treated
387 samples were collected, and a plaque assay was performed to determine the infectious viral titer.

388 The clear zone indicates the plaques formed. (C) Percent inhibition of SARS-CoV-2 replication by
389 3D8 in Vero E6 cells. Vero E6 cells were infected with SARS-CoV-2, and 3D8 was added at 2 hpi.
390 Replication was measured through quantification of the virus RNA level. (D) Cytotoxicity testing
391 of 3D8 in Vero E6 cells was performed by applying a range of 3D8 concentrations in uninfected
392 cell cultures. Error bars indicate the standard deviation of triplicate measurements in a
393 representative experiment. (***) $p < 0.001$, One-way ANOVA test; ns: non-significant)

394

395 **Fig 2. Prophylactic and therapeutic antiviral effects of 3D8 against COVID-19**

396 (A) Inhibition of SARS-CoV-2 by 3D8 in pretreated cell cultures. Vero E6 cells pretreated with
397 3D8 were infected with SARS-CoV-2. At 48 hpi, the cells were harvested, and the viral copy
398 number was quantified based on the relative concentration of the N gene. (B) Vero E6 cells
399 pretreated with 3D8 were infected with SARS-CoV-2. At 48 hpi, the cells were lysed using RIPA
400 lysis buffer. Cell lysates were electrophoresed on SDS-PAGE and transferred to nitrocellulose
401 membranes. After incubation with primary antibodies, the membranes were observed using a
402 chemiluminescence reader. (C) Supernatants were harvested from 3D8-pretreated cell cultures
403 infected with SARS-CoV-2, and the infectious viral titer was determined using a plaque assay. The
404 clear zone indicates the plaques formed. (D) Inhibition of SARS-CoV-2 by 3D8 in post-treated cell
405 cultures. Vero E6 cells were infected with SARS-CoV-2 and treated with 3D8 at 2 hpi. At 48 hpi,
406 the cells were harvested, and the viral copy number was quantified based on the relative
407 concentration of the N gene. (E) Vero E6 cells were infected with SARS-CoV-2 and treated with
408 3D8 at 2 hpi. At 48 hpi, the cells were lysed with RIPA lysis buffer. Cell lysates were
409 electrophoresed on SDS-PAGE and transferred to nitrocellulose membranes. After incubation with
410 primary antibodies, the membranes were observed using a chemiluminescence reader. (F)

411 Supernatants were harvested from 3D8 post-treated cell cultures infected with SARS-CoV-2, and
412 the infectious viral titer was determined using a plaque assay. The clear zone indicates the plaques
413 formed. (**p<0.001; ****p<0.0001, One-way ANOVA test; ns: non-significant)

414

415 **Fig 3. *In vitro* antiviral effect of 3D8 against human coronavirus OC43**

416 (A) Dose-dependent inhibition of OC43 by 3D8. Vero E6 cells were infected with OC43 and treated
417 with a range of 3D8 concentrations at 2 hpi. At 48 hpi, the cells were harvested, and the virus copy
418 number was determined via qPCR. (B) Vero E6 cells were infected with OC43 and treated with
419 3D8 at 2 hpi. At 48 hpi, the cells were lysed with RIPA lysis buffer. Cell lysates were
420 electrophoresed on SDS-PAGE and transferred to nitrocellulose membranes. After incubation with
421 primary antibodies, the membranes were observed using a chemiluminescence reader. (C) Percent
422 inhibition of OC43 replication by 3D8 in Vero E6 cells. Vero E6 cells were infected with OC43,
423 and 3D8 was added at 2 hpi. Replication was measured through quantification of the virus RNA
424 level. (D) Vero E6 cells were treated with OC43 and treated with 3D8 at 2 hpi. At 48 hpi, the cells
425 were washed with PBS and fixed using methanol. Then, they were permeabilized with buffer and
426 blocked with BSA. The cells were then incubated with primary antibodies overnight. After
427 incubation, TRITC-conjugated anti-mouse and Alexa 488-conjugated anti-rabbit antibodies were
428 added. Hoechst was used to stain the nucleus. (*p< 0.05; ***p<0.001, One-way ANOVA test; ns:
429 non-significant)

430

431 **Fig 4. *In vitro* antiviral effect of different concentrations of 3D8 against PEDV**

432 (A) Dose-dependent inhibition of PEDV by 3D8. Vero E6 cells were infected with PEDV and
433 treated with a range of 3D8 concentrations at 2 hpi. At 48 hpi, the cells were harvested, and the

434 virus RNA level was determined via qPCR. (B) Vero E6 cells were infected with PEDV and treated
435 with 3D8 at 2 hpi. At 48 hpi, the cells were lysed with RIPA lysis buffer. Cell lysates were
436 electrophoresed on SDS-PAGE and transferred to nitrocellulose membranes. After incubation with
437 primary antibodies, the membranes were observed using a chemiluminescence reader. (C) Percent
438 inhibition of PEDV replication by 3D8 in Vero E6 cells. Vero E6 cells were infected with PEDV
439 and treated with 3D8 at 2 hpi. Replication was measured through quantification of the virus RNA
440 level. (D) Vero E6 cells were treated with PEDV and treated with 3D8 at 2 hpi. At 48 hpi, the cells
441 were washed with PBS and fixed with methanol. Then, they were permeabilized with buffer and
442 blocked with BSA. The cells were incubated with primary antibodies overnight. After incubation,
443 TRITC-conjugated anti-mouse and Alexa 488-conjugated anti-rabbit antibodies were added.
444 Hoechst was used to stain the nucleus. (* $p < 0.05$; ** $p < 0.01$, One-way ANOVA test; ns: non-
445 significant)

446

447 **Fig 5. Suggested mode of action for 3D8**

448 3D8, a single chain variable fragment (scFv), is internalized into the cell through caveolae-mediated
449 endocytosis. After release from the endosomal compartment, 3D8 localizes to the cytosol. In the
450 cytosol, it binds to the viral nucleic acid and degrades it to prevent its amplification, thus inhibiting
451 viral growth. 3D8 confers nuclease activity without sequence specificity and hydrolyzes viral RNA
452 genomes or transcripts.

453

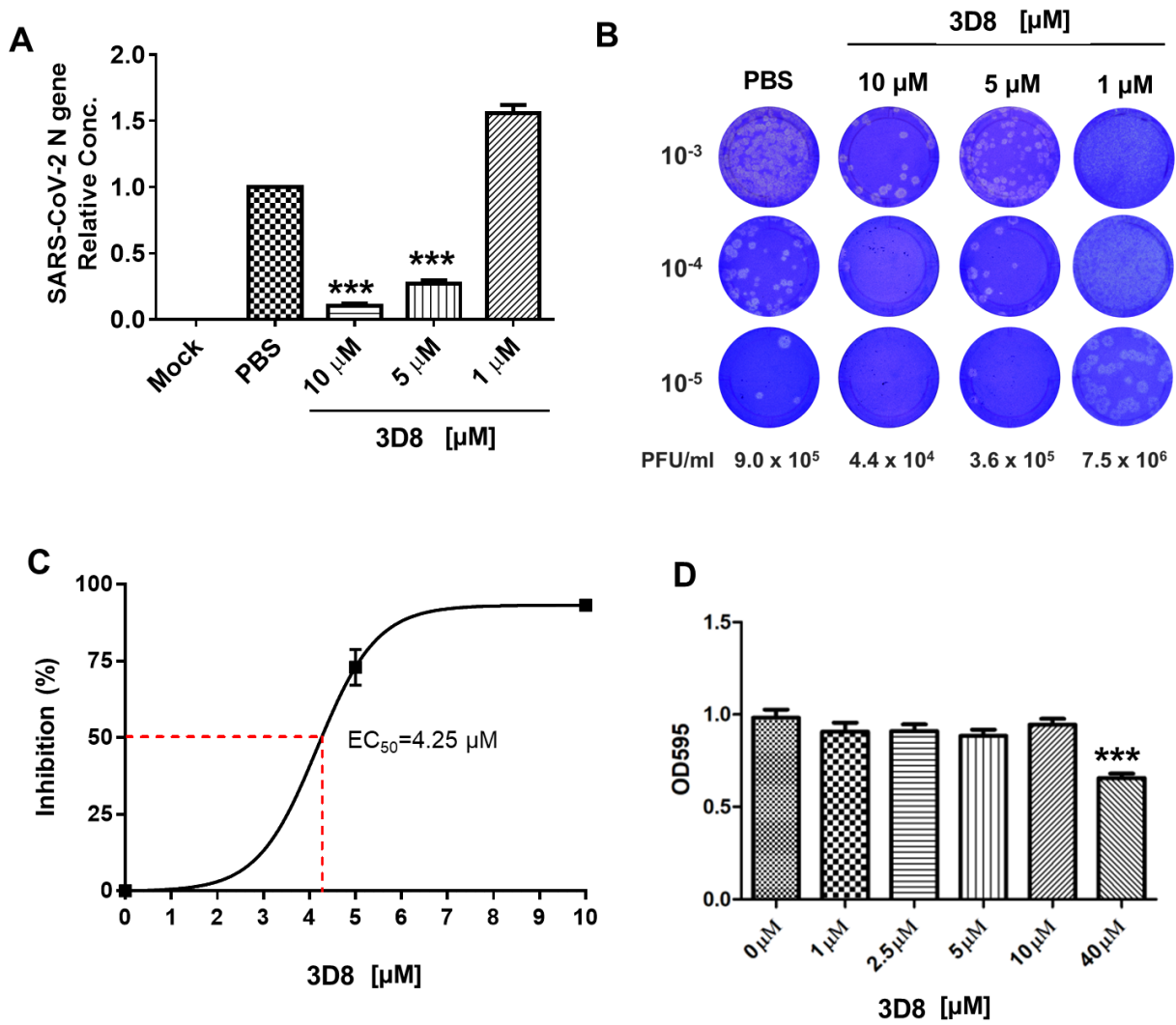
454

455

456

457 **Figures.**

458 **Fig 1.**



459

460

461

462

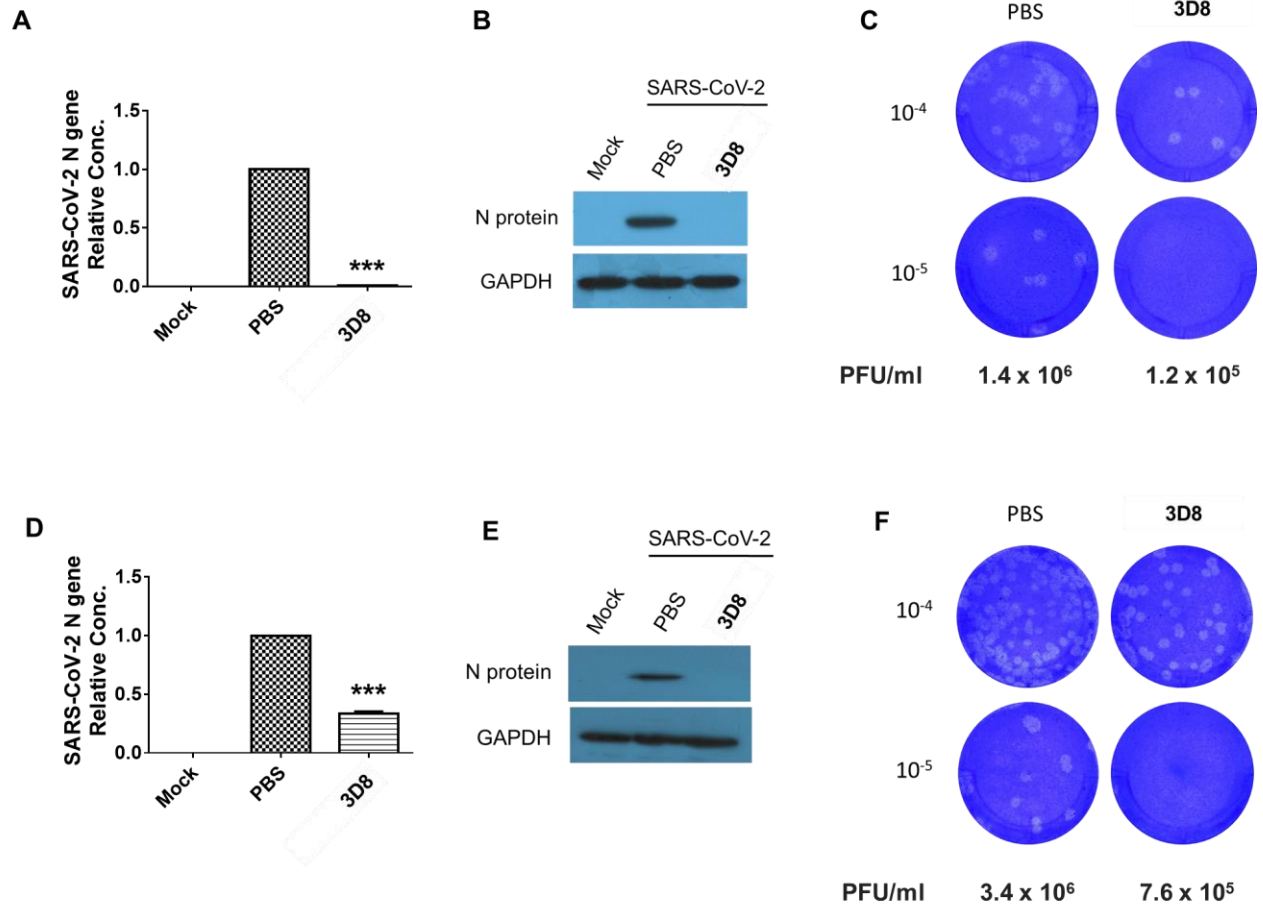
463

464

465

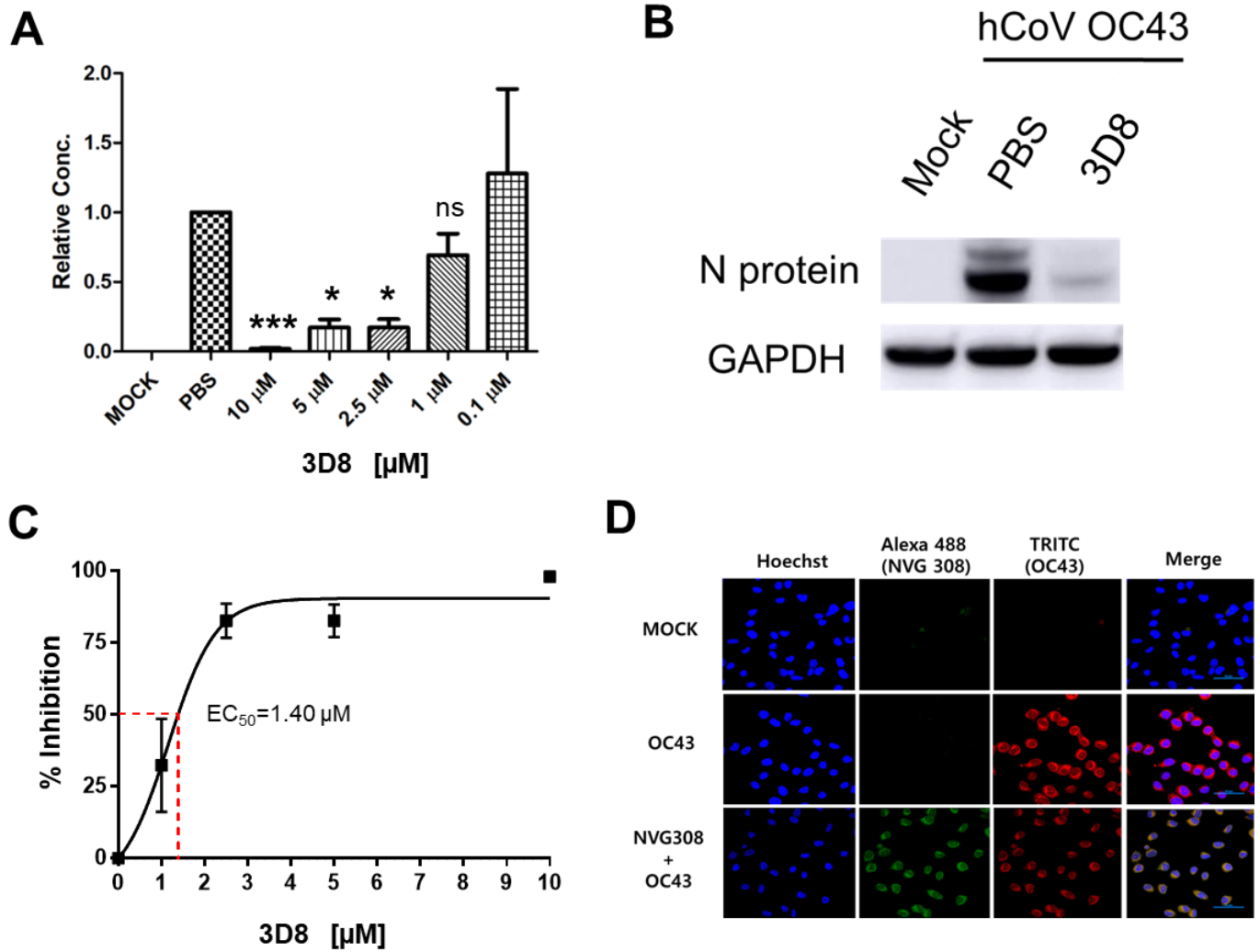
466 **Fig 2.**

467



468

469 **Fig 3.**



470

471

472

473

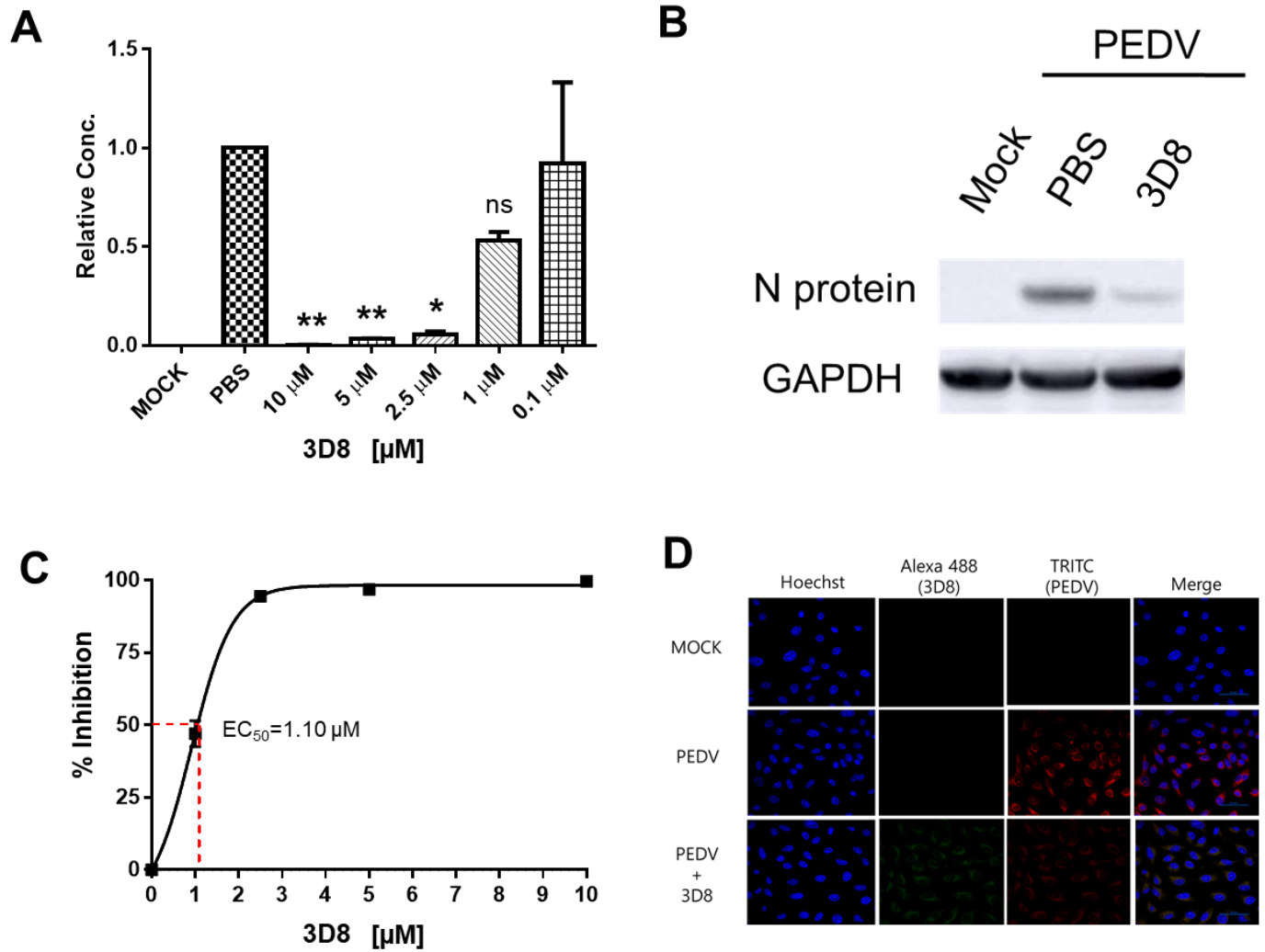
474

475

476

477

478 **Fig 4.**



479

480

481

482

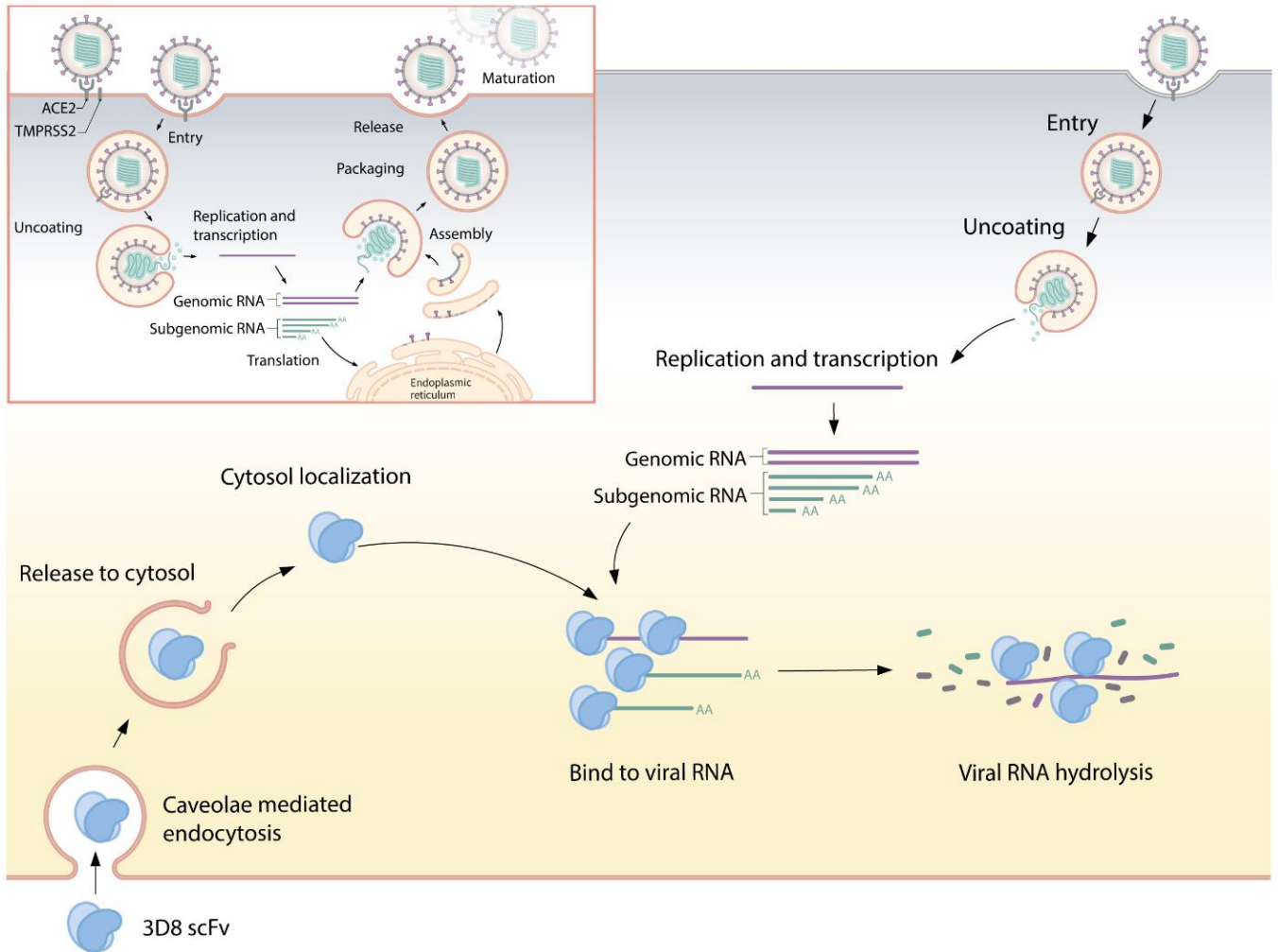
483

484

485

486

487 **Fig 5.**



488